Costs and Benefits of Social Relationships in the Collective Motion of Bird Flocks

Hangjian Ling[1], Guillam E. Mclvor[2], Kasper van der Vaart[1], Richard T. Vaughan[3], Alex Thornton[2]*, Nicholas T. Ouellette[1]*

[1]Department of Civil and Environmental Engineering, Stanford University, Stanford, CA USA;

[2]Center for Ecology and Conservation, University of Exeter, Penryn, UK;

[3]School of Computing Science, Simon Fraser University, Burnaby, Canada

Correspondence: Nicholas T. Ouellette (e-mail: nto@stanford.edu), Alex Thornton (e-mail: alex.thornton@exeter.ac.uk)

Current understanding of collective behaviour in nature is based largely on models assuming identical agents obeying the same interaction rules, but in reality interactions may be influenced by social relationships between group members. Here, we show that social relationships transform local interactions and collective dynamics. We tracked individuals' 3D trajectories within flocks of jackdaws, a bird that forms lifelong pair-bonds. Reflecting this social system, we find that flocks contain internal sub-structure, with discrete pairs of individuals tied together by spring-like effective forces. Within flocks, paired birds interacted with fewer neighbours than unpaired birds and flapped their wings more slowly, which may result in energetic savings. However, flocks with more paired birds had shorter correlation lengths, which is likely to inhibit efficient information transfer through the flock. Similar changes to group properties emerge naturally from a generic self-propelled particle model. These results reveal a critical tension between individual- and group-level benefits during collective behaviour in species with differentiated social relationships, and have significant evolutionary and cognitive implications.

Collective behaviour occurs throughout nature and conveys numerous benefits, from predator avoidance to social learning[1,2]. Numerous theoretical models have shown that simple rules for local interaction among individuals can generate coordinated, cohesive group behaviour similar to that found in natural systems ranging from microbial mats to the spectacular displays of fish schools, bird flocks, and even human crowds[2–4]. Following the traditional and successful paradigms of statistical physics, models typically assume that the individuals that make up these groups are identical. In nature, however, group members may vary substantially in their individual characteristics and social relationships[5,6]. As such, existing modeling paradigms may be unable to address broader ecological and evolutionary questions[7]. Recently, therefore, researchers have begun to emphasize the role of individual differences, showing that accounting for individual variation in local interaction rules can change group behavior[6,8]. The differentiated social relationships that characterize many animal societies are particularly likely to influence collective dynamics[9], because individuals in many species, including many birds[10,11], mammals[12] and, of course, humans[13], are frequently observed to stay close to and move together with those with whom they share a strong social affiliation. Computational models of collective movement incorporating social network structure[5] suggest that social relationships can modify the spatial positions of individuals within groups[14] as well as overall group cohesion[15,16] and polarization[16,17]. However, empirical data on the effect of social relationships on interaction rules and group behaviour remains very limited[13,15,18]. Critically, no study has examined how the existence of differentiated social relationships within groups influences the energetics and dynamics of group movement or the transmission of information through the group.

Bird flocks are among the best studied and most spectacular examples of collective behaviour in nature. However, although many avian societies contain long-term, stable relationships such as reproductive pair bonds[19], theoretical[20,21] and empirical[22,23] research has largely ignored the impact of social bonds on flocking. Jackdaws, a highly social corvid species, form life-long monogamous pair bonds, and bonded partners remain in close proximity throughout the year[24–28] (see Methods for further details). These close bonds are reflected in winter flocks, where photographic snapshots show that individuals commonly fly particularly close to one other flock member[11]. Here, we investigate how pairing influences individual movement interactions, flight performance, and group-level properties of flocks. We recorded and tracked the three-dimensional (3D) movement of wild jackdaws in six flocks for periods of 3 to 5 seconds (Supplementary Table 1; Supplementary Videos 1 to 6; Supplementary Data 1 to 6) using a high-speed stereo-imaging system[29]. We measured the time-resolved position $\boldsymbol{x}^i=(x_1^i, x_2^i, x_3^i)$, velocity $\boldsymbol{u}^i=(u_1^i, u_2^i, u_3^i)$, acceleration $\boldsymbol{a}^i=(a_1^i, a_2^i, a_3^i)$, and wingbeat frequency f_{wb}^i of each bird *i* in a Cartesian coordinate system where $-x_3$ points in the direction of gravity and $+x_1$ is the time-averaged flight direction of the flock. The instantaneous 3D distributions of birds are shown in Fig. 1a and Supplementary Fig. 1. We label the distance from a focal bird *i* to its n^{th} nearest neighbour as $D^{i,n} = |\boldsymbol{x}^{\boldsymbol{i}}-\boldsymbol{x}^{\boldsymbol{i,n}}|$, where $\boldsymbol{x}^{\boldsymbol{i,n}}$ is the position of the n^{th} nearest neighbour.

Results and Discussion

First, we confirm that, contrary to existing flocking models that assume a homogeneous distribution of individuals in a group[20,21], discrete pairs exist within these flocks. Strong statistical evidence for pairing is seen in the radial distribution function $G(r)$, which measures the normalized likelihood of finding a neighbour a distance *r* away from a focal bird. In jackdaw flocks, $G(r)$ consistently shows a peak for values of *r* smaller than the mean nearest-neighbour distance $<D^{i,n=1}>$ (Fig. 1b, Supplementary Fig. 1), indicative of a substantial number of birds that fly anomalously close together. Here, the symbol < > denotes an ensemble average over different birds. We find additional evidence for pairing by examining the joint probability density functions (PDFs) of $D^{i,n=1}$ and $D^{i,n=2}$ (Fig. 1c, Supplementary Fig. 1), which show two distinct regions of high probability that we label as lobes I and II. In lobe I, $D^{i,n=1}$ increases proportionally with $D^{i,n=2}$, but in lobe II $D^{i,n=1}$ remains small even as $D^{i,n=2}$ increases (thereby reducing local density). Both the small-*r* peak in $G(r)$ and the presence of lobe II in the joint PDFs are consistent with the existence of pair-bonded birds who remain close together regardless of other conditions in the flock. We therefore define two birds *i* and *j* to be paired if their separation distance is smaller than

$(1/2)^{0.5} \times min\{D^{i,n=2}, D^{j,n=2}\}$ when averaged along their entire measured trajectories (see *Methods* for details). The instantaneous percentage of paired birds P_{paired} ranges from 5% to 80% (Supplementary Table 1).

After discriminating between paired and unpaired birds, we studied how pairing affects the local interactions between individuals. We find that unpaired birds tend to exchange neighbours slowly, while paired birds maintain a nearly fixed distance to their partners (Fig. 2a, Supplementary Fig. 2). Paired birds exhibited a spring-like response to their partners[30], with acceleration increasing linearly with distance (Fig. 2b, Supplementary Fig. 2). In contrast, the long-range attraction was much weaker between unpaired birds and their nearest neighbours, likely because they responded equally to multiple neighbours (see next paragraph)[30].

Typical flocking models assume that all individuals, regardless of their identity, have the same interaction range, whether topological (that is, a number of neighbours)[20,21] or metric (that is, a distance in space)[3]. In contract, we find that the interaction range depends strongly on whether the focal bird is paired or not. Following the method used for analysing starling flocks[22], we calculated the topological interaction range by measuring the anisotropy factor γ (see *Methods*) of the spatial distribution of a focal bird's n^{th} neighbour. Empirically, γ decreases with the topological rank n; we define the interaction range at which γ reaches its isotropic value (γ=0). For unpaired birds, we find that individuals interact with 7 or 8 neighbours on average (Fig. 2c), similar to what has been found for starlings[22]. However, for paired birds, the magnitude of $\gamma(n=1)$ was much higher than for unpaired birds and γ decreased to 0 at a faster rate, with $\gamma(n=3 \text{ or } 4) \approx 0$ (Fig. 2c). This finding indicates that paired birds have a reduced interaction range, interacting with only half as many neighbours as their unpaired conspecifics. This interpretation is consistent with our measurements of the alignment of birds with their neighbours, as we find that paired birds align less well than unpaired birds with their neighbours (excluding n=1) (Fig. 2d, Supplementary

Fig. 2). This smaller interaction range may possibly be due to the additional cognitive constraints associated with having to keep track of and respond to one specific partner among the crowd. In addition to social relationships, individual variations such as a propensity to be found near the group center have also been reported to affect interaction ranges[8].

As the reproductive costs of losing a partner are substantial, birds with long-term, monogamous pair-bonds may benefit from keeping track of their partner throughout the year, even when flying within dense flocks[11,19,24]. Given that paired birds respond to the movements of fewer neighbours within flocks compared to unpaired birds (Fig. 3a), it is also possible that flying in pairs provides energetic benefits. To investigate this, we compared the flight performance of paired and unpaired birds flying in flocks and alone ("alone" being defined as having $D^{i,n=2}$>5 m), all in the same cruising flight mode[29] defined by $|u_3|$<1 m/s and $|\boldsymbol{a}|$<5 m/s^2. Since we did not measure birds' metabolic rates, we estimated the power output in flight via the wingbeat frequency[31,32] (measured by applying a continuous wavelet transform to the wing motion[29]; see *Methods*). According to the measurements of similarly sized birds by Tobalske *et al*. (2003)[32], an increase of f_{wb} is highly correlated with an increase of mechanical power output at flight speed of $|\boldsymbol{u}|$>10 m/s. Given the similarity in size between jackdaws and the birds studied by Tobalske *et al*. (2003)[32], it is reasonable to assume that the relationship between f_{wb} and mechanical power are similar here. For $|\boldsymbol{u}|$>10 *m/s*, birds flying in flocks had a higher f_{wb} compared to those flying in isolation (Fig. 3b; ANOVA: $F_{2,886}$ = 14.07, r =0.17, p<0.001; Supplementary Table 2; Supplementary Data 8), suggesting that flocking is energetically costly, consistent with previous results for pigeons[31]. One possible reason, as has been proposed previously[29,31], is that birds have to coordinate with others in group flight and manoeuvre more rapidly to avoid collisions. If this explanation were true, we would expect that when flying in flocks, pairing would lead to a reduction in energy consumption due to the reduced interaction range. Indeed, we find that the magnitude of f_{wb} for paired birds in groups is lower than for unpaired birds at $|\boldsymbol{u}|$>10 m/s (Fig. 3b; Supplementary Fig. 3; Supplementary Table 3; Supplementary Data 8). Such differences are not caused by local density effect[29] since paired birds can fly either in denser or sparser regions within flocks (Supplementary Fig. 4). Thus, flying with a partner appears to provide important energetic benefits relative to being unpaired within flocks.

Next, we investigated how the presence of pairs within flocks affects the potential sensitivity of the flock as a whole. The ability of animal groups to respond collectively to perturbations such as predator attacks depends on the efficient transfer of information, so that individual changes in behaviour spread through the whole group[2,23]. One indicator of efficient information transfer is a large velocity correlation length[20,23,33,34]. We therefore calculated the correlation functions of the velocity fluctuations $C(r)$, and defined the correlation length r_0 by $C(r=r_0)=0$[23] (see *Methods*). Sample velocity fluctuations and correlations are shown in Figs. 4a and 4b. At small r, C is greater than 0, meaning that a change in the velocity of an individual is associated with similar changes for other group members separated by those distances. As r increases, C slowly decays, indicating that the motion of birds separated by larger distances is less similar. The distance r_0 at which C drops to 0 quantifies the range of this similarity, and thus is an indicator of how efficiently behavioral changes by some individuals propagate through the group. Comparing different flocks reveals that increasing P_{paired} leads to a shorter r_0/L, where L is the group size (Fig. 4c, Pearson's correlation=0.32, $p<0.001$). The scatter we observe is likely primarily due to less than ideal convergence of the correlation functions computed for individual frames of data, as opposed to being averaged over many different time steps (see Supplementary Fig. 5), with some potentially additional influence of different external environmental conditions. To test whether this trend may apply more generally to any biological system where individuals exhibit different interaction ranges, we ran a simple model of self-propelled particles using only alignment and repulsion rules[3,35] (see *Methods*). We observe the same trend in this model (Fig. 4c). Thus, the presence of social pairs within flocks appears to impose a cost on all flock members by inhibiting efficient information transfer. This is likely to increase individuals' vulnerability to, for example, predator attacks[23]. As currently available data does not allow us to quantify explicitly how the reduction of correlation length affects the speed and accuracy of information transfer, the precise value of global cost due to social relations remains unknown.

Future modeling and experimental work is necessary to specify the details of this cost. We also found that increasing P_{paired} reduces group density (Pearson's correlation=0.72, $p<0.001$) and group polarization (Pearson's correlation=0.18, $p<0.05$) (Supplementary Fig. 6), which may also reduce group cohesion and introduce additional costs for flock members.

Conclusions

Our findings suggest that social bonds have significant impacts on the structure and function of flocks, and therefore have important cognitive and evolutionary implications. Research in collective behaviour typically treats flocking animals as "mindless" agents following identical rules, but our results suggest that jackdaws may face substantial cognitive demands to recognise and keep track of their partner among the crowd. As jackdaws are highly vocal when flocking, these are likely to include the need to recognise their partner's calls within a noisy environment and potentially integrate acoustic and visual cues of individual identity[36,37]. Similar cognitive demands of collective behaviour are likely to be widespread in species with stable social relationships. From an evolutionary perspective, we reveal a hitherto unrecognised conflict of interest: maintaining social bonds during flocking benefits paired individuals, but imposes a cost of reduced sensitivity to the environment for the flock as a whole. Determining how such conflicts are resolved is now critical for our understanding of the evolution of flocking and flock composition.

Figures Legends

Fig. 1 | Flock morphology and evidence of pairing. a, Spatial distributions and velocities of birds in three-dimensional space. Paired birds are coloured in red. **b**, Radial distribution functions $G(r)$ showing peaks for r smaller than $\langle D^{i,n=1} \rangle$. **c**, Joint PDFs of $D^{i,\,n=1}$ and $D^{i,\,n=2}$, showing two lobes of high probabilities: lobe I corresponds unpaired birds; and lobe II represents paired birds. All data are from flock #1 (data from other flocks are shown in Supplementary Fig.1).

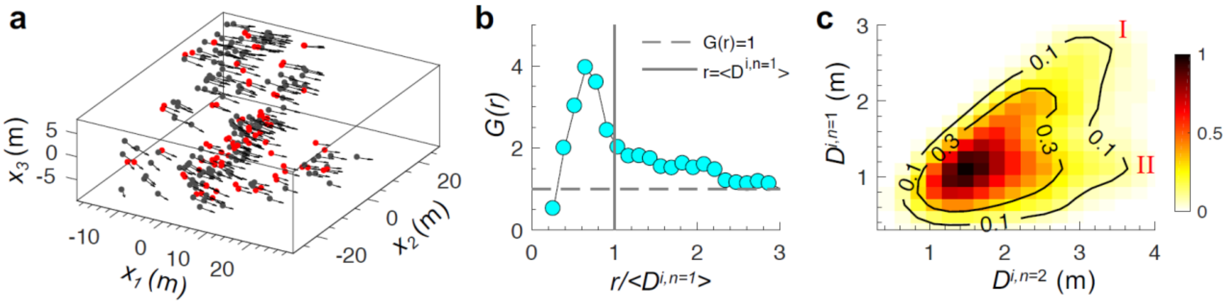

Fig. 2 | Pairing causes variations in local interaction. a, Change of distance between a bird and its nearest neighbour at time 0. **b**, Acceleration in the direction away from the nearest neighbour; positive values are repulsive and negative values are attractive. **c**, Anisotropy factor γ of the spatial distribution of the n^{th} neighbour. $\gamma>0$ indicates a higher probability of finding a neighbour next to rather than in front or back of the focal bird. **d**, Alignment angle between a focal bird and its n^{th} neighbour. All data are from flock #1 (data from other flocks are shown in Supplementary Fig. 2). Standard errors are smaller than the symbols.

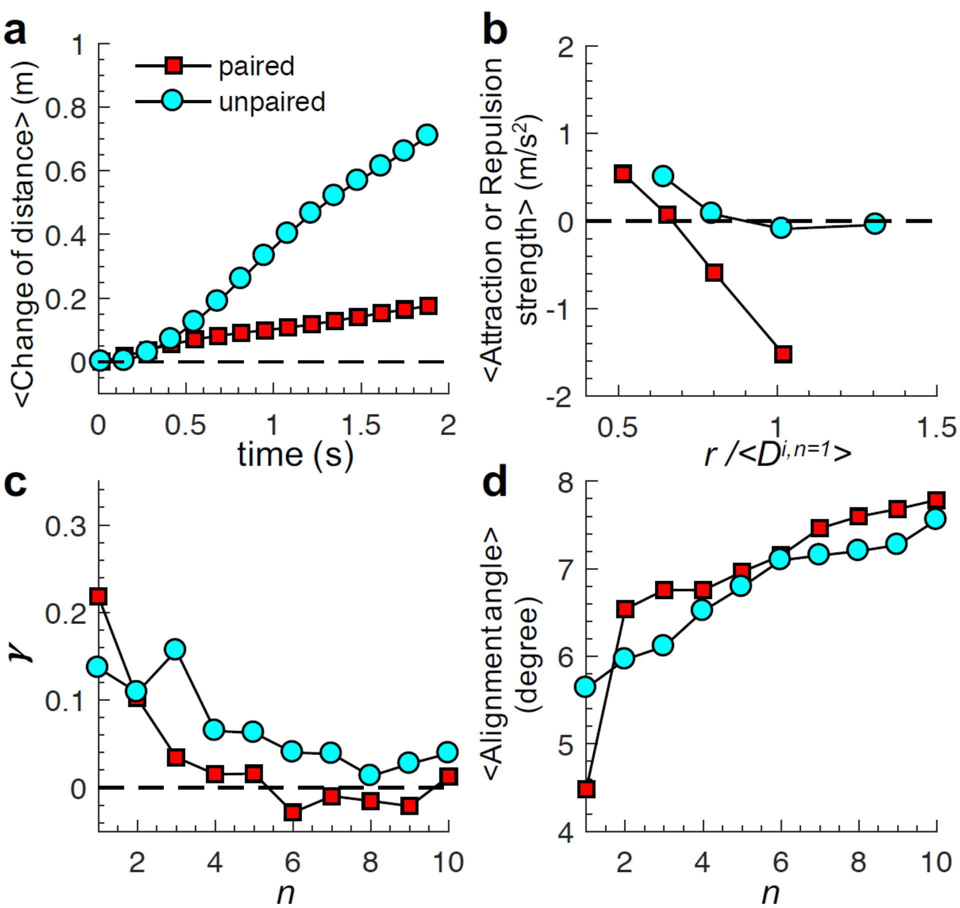

Fig. 3 | Effect of pairing on the power consumption of individuals. a, Illustrations of interaction networks of focal birds. Lines indicate interactions between birds. **b**, Wingbeat frequency f_{wb} as a function of flight speed $|\boldsymbol{u}|$ during cruising flight mode. Each data point for birds in group is calculated by averaging more than 800 measurements in flock #1 (data from other flocks are shown in Supplementary Fig. 3). Data for birds flying alone are calculated by averaging 64 jackdaws. Standard errors are smaller than the symbols. The magnitudes of $|\boldsymbol{u}|$ represent ground speeds.

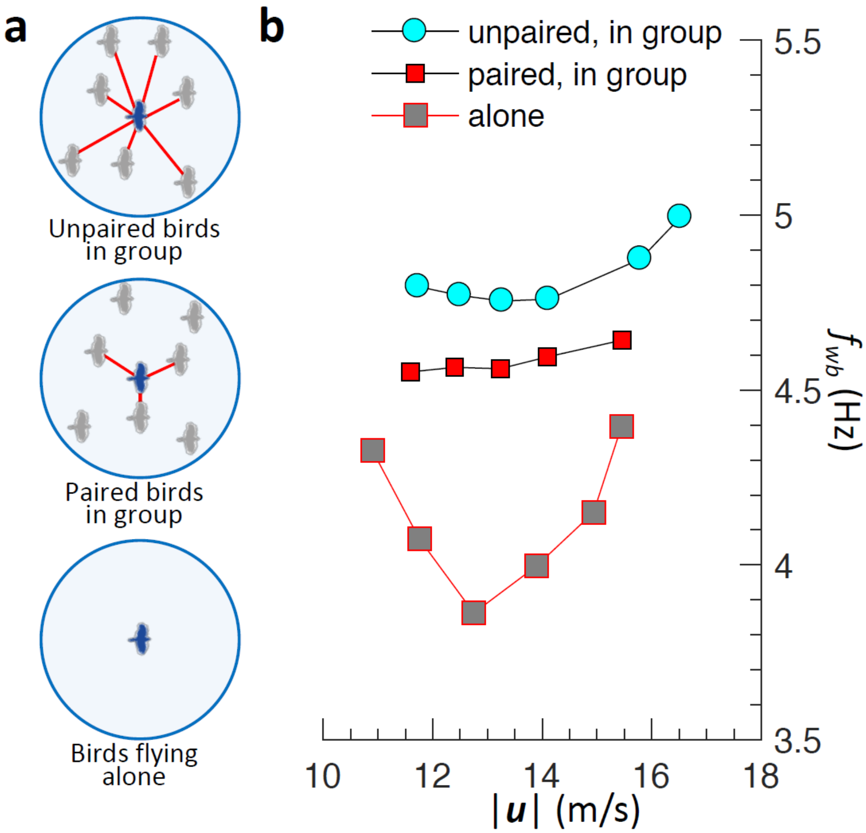

Fig. 4 | Pairing reduces group correlation lengths. a, Sample instantaneous velocity fluctuations (taken from flock #1) projected onto the horizontal plane (x_1, x_2). **b**, Velocity correlation function $C(r)$ for the data shown in **a**. **c**, Correlation length r_0 as a function of P_{paired}, where each data point is for one time frame for a given flock. Here, r_0 is normalized by group size L=max{$D^{i,n}$}.

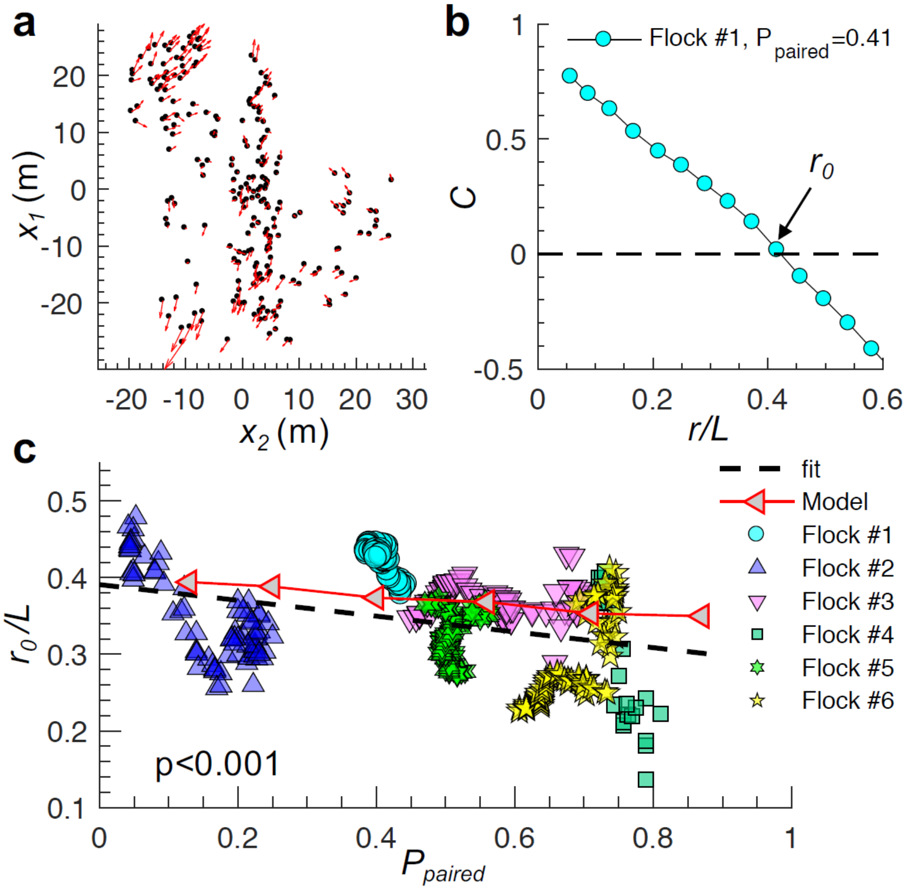

Methods

Study system. Jackdaws (*Corvus monedula*) are a highly social, colony-breeding corvid found throughout much of the Western Palaearctic. Individuals form long-term (commonly lifelong), monogamous relationships and both parents contribute to rearing the young[26,38,39]. During the winter months, large numbers of individuals, including mated pairs, unpaired individuals and juveniles leave their foraging grounds in the early evening and aggregate in flocks that then fly towards roosts (often with staging stops at pre-roost trees) where they spend the night. Jackdaws often form mixed-species flocks with rooks (*Corvus frugilegus*)[11], but to avoid any confounds caused by species differences the analyses in this paper used only flocking events in which all flock members were jackdaws (identified by vocalisations and morphological characteristics). Further criteria for inclusion in the analyses were (i) a minimal flock size of at least 78 individuals to allow robust measures of local density and interaction; (ii) flock images were captured by all four cameras; and (iii) flocks were moving primarily in one direction without making large-scale turns.

At our study sites in Cornwall, U.K., more than 2000 jackdaws are fitted with unique colour ring combinations for individual identification. Although colour rings are not visible within our images of birds in flight, we are confident that the pair-wise interactions we identify within flocks reflect pair-bonded mates flying together. First, data from our own and other study sites shows that pair-bonded birds remain in close proximity to each other throughout the year[24–28]. In previous studies[26,40], paired jackdaws have regularly been observed to depart together from nests, perching positions and foraging grounds, including at times when winter flocks are setting off towards their roosting sites. In addition, we frequently see isolated pairs of birds flying together (Ling *et al.*, 2018)[29] (for instance, in an eight-week period during the winter of 2017/18, we recorded more than 300 isolated pairs; Supplementary Data 7). Moreover, jackdaws are known to discriminate between the calls of different conspecifics[36,41] and are highly vocal in flight, particularly when flying within large flocks. The ability to distinguish a partner's voice among the cacophony calls (the "cocktail party effect[42]") is therefore likely to be critical in allowing paired birds to keep track of each other, potentially aided by the integration of acoustic and visual cues of individual identity[43].

Camera setup and calibration. To track the three-dimensional (3D) movements of birds, we used a stereo-imaging system with four cameras (Basler ace acA2040-90um, pixel size of 5.5 µm, sensor resolution of 2048 by 2048 pixels, up to 90 frames per second) mounted on tripods. A typical arrangement of the four cameras is shown in Supplementary Fig. 7a. Two pairs of cameras were separated by 50~60 m. The distance between each camera in a pair was 8~10 m. All cameras pointed to the sky with an angle to the horizontal plane of 60 degrees. We connected each pair of two cameras to one laptop (Thinkpad P51 Mobile Workstation) via USB 3.0 ports. The laptops provided power to the cameras and served as data storage device (512 GB Solid-State Drive, and 2 TB Hard Drive). The four cameras were precisely synchronized by external signals generated by a function generator (Agilent 33210A). Each camera was fitted with a lens with a focal length of 8 mm and an angle of view of 71 degrees (Tamron, M111FM08). The system was able to image an area of 60 by 60 m^2 with uncertainty of 4.0 cm/pixel at a height of 50 m. The overall imaging system is very portable and can be moved easily from one location to another on different days to ensure the capture of flock images.

Stereo-imaging relies on matching the two-dimensional (2D) coordinates of an object as recorded on multiple cameras[44]. A stereo-matching procedure requires knowledge of camera parameters such as positions and orientations (extrinsic parameters) and focal lengths and principle points (intrinsic parameters). We followed a procedure developed by Theriault *et al*. (2014)[45] to determine these camera parameters. First, we flew a drone that carried two balls of different sizes (10 and 12 cm) through the tracking volume. The distance between the two balls was fixed at 1 m, which provided a physical scale for our calibration. We recorded a series of images of the two balls on each of the four cameras as the drone flew through the tracking volume. Then, we determined the locations of balls in each 2D image and generated more than 300 sets of matched points between the cameras. Using these matched 2D points, we approximated the fundamental matrix of each camera and the 3D positions of the matched points using the eight-point algorithm[44]. Finally, the camera parameters were refined by sparse bundle adjustment[46]. A sample illustration of the 3D calibration points and camera positions is shown in Supplementary Fig. 7b.

Data collection. We recorded flocks of jackdaws flying towards winter roosts in Mabe and Gwennap, Cornwall, UK from December 2017 to March 2018. The birds typically left their foraging grounds in the late afternoon (when pair-bonded mates are often seen together) and merged as they flew towards pre-roosts or roosting assembly points. Since the flight trajectories were quite predictable, we were able to position the camera system at locations where flocks would fly overhead. The flock typically flew at a height of ~50 m with flight speeds of 10~18 m/s. We were able to continuously track the flock for 3~5 seconds with a recording rate of 60 frames per second. We thus obtained 180~300 frames for each flocking event; six events were analysed in this paper. Wind speeds were typically below 4.5 m/s. We assumed that birds in the same flock experienced similar wind speeds, particularly after averaging over a few seconds. We thus neglect the wind speed in our data analysis and only report the group speed. Since our recording time duration is longer than time scale for unpaired birds to exchange neighbours (<2 seconds, Fig. 2a, Supplementary Fig. 2), the tracking results are highly likely to capture typical flock movement. Indeed, ornithologists have long noted that the presence of discrete pairs flying together within jackdaw flocks is clearly evident even to the naked eye[40].

Three-dimensional reconstruction and tracking. To calculate individual 3D trajectories of birds, we first located the birds on each image. Distinct blobs of pixels corresponding to birds were segmented by setting a global intensity threshold on images after subtracting the mean background averaged over 50 temporally consecutive images. For each blob, we calculated the intensity-weighted centroid and treated it as 2D location of a bird.

We matched the 2D coordinates belonging to the same object across all four cameras to reconstruct the 3D world coordinates through triangulation. The matching process involved finding candidates located within a small tolerance of the epipolar lines. Supplementary Fig. 8 shows sample epipolar lines projected on camera 3, where each epipolar line crosses one or more birds. These matched candidates are combined to calculate the 3D locations using a least-squares solution of the line-of-sight equations[44]. When multiple 3D positions for the same bird are possible, we select the one with the smallest 3D ray intersection distance (that is, the residual of the least-squares solution). The ray intersection distances for the best matches were typically smaller than 0.3 m (about half of birds' body size). When re-projecting the reconstructed birds' 3D positions back onto 2D images, they overlapped with the bird images (Supplementary Fig. 8). We solved the optical occlusion problem by associating every detected bird on each camera with a 3D position. Further details of the stereo-imaging procedures are given in Ling *et al.* (2018)[29].

We linked the 3D locations belonging to the same object over multiple time frames based on a three-frame predictive particle tracking algorithm that used estimates of both velocity and acceleration[47]. This algorithm has been proven to perform well in intense turbulent flow[48] and midge swarms[49]. The velocities and accelerations were calculated by convolving the trajectories with a Gaussian smoothing and differentiating kernel[50].

Measurement of wing motion and wingbeat frequency. Following a method developed in our previous work[29], we measured the wing motion and time-varying wingbeat frequency of each bird along their 3D trajectories. First, we detected the intensity-weight centroids of each bird on images to approximate the birds' 2D positions (Supplementary Fig. 9a). These 2D locations included both the low-frequency body motion and higher-frequency wing motion. Thus, the reconstructed 3D trajectories based on these 2D measurements included information from both body and wing motion (Supplementary Fig. 9b). Here, the term body motion refers to the change of the bird center of mass when ignoring the wing flap induced body oscillation, and thus the body acceleration in the gravity direction only measures the change of potential energy. Since the body and wing motions have well separated frequencies, however, we were able to separate them in the frequency domain. We obtained the body motion by applying a cut-off frequency in measured acceleration and then integrating the filtered acceleration (Supplementary Fig. 9c). By re-projecting the calculated body positions back onto the 2D images, we confirmed that the calculated body motion indeed accurately represented the bird movement (Supplementary Fig. 9e). The wing motion was then obtained by subtracting the body motion from the measured trajectories (Supplementary Fig. 9d). Finally, the wingbeat frequency was obtained by applying a continuous wavelet transform[51] to the wing motion (Supplementary Fig. 9f). As shown in Supplementary Fig. 9g, we were able to measure the wingbeat frequency along the birds' 3D trajectories. This sample trajectory shows a bird transitioning from flapping flight to gliding flight.

Identification of paired and unpaired birds. Since we have shown strong evidence for the existence of discrete pairs in the flock, we developed a criterion to identify birds that belong to discrete pairs. We found that the average distance to the nth nearest neighbour follows the power law $\langle D^{i,n}\rangle \sim n^{0.5}$ for $n>1$. The power exponent is very close to 0.5, indicating that birds are roughly distributed on a two-dimensional plane. However, due to the existence of discrete pairs, $\langle D^{i,n=1}\rangle$ is lower than the power law prediction. Therefore, paired birds must satisfy $D^{i,n=1}/1^{0.5} < D^{i,n=2}/2^{0.5}$, and unpaired birds have $D^{i,n=1}/1^{0.5} \sim D^{i,n=2}/2^{0.5}$. Thus, we define two birds i and j to be socially paired if their distance $D^{i,j}$ satisfies the criterion $D^{i,j}<(1/2)^{0.5}\times min\{D^{i,n=2}, D^{j,n=2}\}$. This criterion is very similar to what has been used in previous work[11]. However, since birds in flocks continuously exchange neighbors[52], an unpaired bird can briefly fly very close to a neighbour and will be falsely identified by this method. Since we continuously tracked the flock movement, we eliminate such false detections by requiring $D^{i,j}$ averaged over the entire measured trajectory to satisfy this criterion, instead of relying only on a single snapshot[11].

Neighbour structure and anisotropy factor. For a focal bird i located at $\boldsymbol{x}^i$ and its n^{th} nearest neighbour located at $\boldsymbol{x}^{i,n}$, we calculated the position of a neighbouring bird relative to the focal bird as $\boldsymbol{p}^{i,n}= \boldsymbol{x}^{i,n}-\boldsymbol{x}^i$. We then translated $\boldsymbol{p}^{i,n}$ into a new coordinate system (ξ,η) where $+\xi$ is the flight direction of the focal bird (ignoring u_3 since $u_3<<u_1$), giving $\xi^{i,n}=(p_1^{i,n}u_1^i+p_2^{i,n}u_2^i)/[(u_1^i)^2+(u_2^i)^2]$ and $\eta^{i,n}=(p_2^{i,n}u_1^i-p_1^{i,n}u_2^i)/[(u_1^i)^2+(u_2^i)^2]$. We repeated this calculation for all the birds within the group. The joint probability density functions (PDFs) of $\xi^{i,n}$ and $\eta^{i,n}$ give the statistics of the spatial position of the n^{th} neighbour. For small topological rank n (n<7) where one would expect interaction, the statistics of this relative location are highly anisotropic (Supplementary Fig. 10, Supplementary Fig. 11a-b), with a higher probability of finding a neighbour next to rather than in front or in back of the focal bird. For higher n (n=8), they become nearly isotropic (Supplementary Fig. 11c), with neighbouring birds distributed randomly in space. To quantify the degree of anisotropy in these structures, we normalized each vector $(\xi^{i,n}, \eta^{i,n})$ to create a unit vector denoted as $(d\xi^{i,n}, d\eta^{i,n})$. We defined the anisotropy factor $\gamma=\langle d\eta^{i,n}d\eta^{i,n}-d\xi^{i,n}d\xi^{i,n}\rangle$. The value of γ ranges from –1 to 1 by construction. $\gamma > 0$ indicates that the neighbouring bird is more likely to be next to the focal bird, $\gamma < 0$ indicates that the neighbouring bird is more likely to be in front or back, and $\gamma = 0$ indicates an isotropic structure where the neighbouring bird is randomly distributed around the focal bird. We also calculated the joint PDFs of $\xi^{i,n}$ and $p_3^{i,n}$ (the height difference between a focal bird and its n^{th} nearest neighbour). The structure in ($\xi^{i,n}$, $p_3^{i,n}$) is more elongated in the ξ direction for larger values of n (Supplementary Fig. 11d-f) since the flocks are relatively thin in the gravity direction. However, defining an anisotropy factor based on ($\xi^{i,n}$, $p_3^{i,n}$) was not as simple as for ($\xi^{i,n}$, $\eta^{i,n}$), and so we opted to use data in the ($\xi^{i,n}$, $\eta^{i,n}$) plane for our analysis. Note that for flocks with fewer than 150 birds (flocks #2-6), the portion of birds on the boundaries is high and may contaminate the statistics. Thus, we did not analyse the neighbour-distribution statistics for these flocks (excluding n=1 shown in Supplementary Fig. 10)

Correlation function and correlation length. For each flock, we calculated the velocity fluctuation of each bird as $\delta\boldsymbol{u}^i=\boldsymbol{u}^i-\langle\boldsymbol{u}^i\rangle$, where the average was taken over all birds within the flock. Following a method used by Attanasi *et al*. (2014)[53], the fluctuations were normalized as $\delta\varphi^i=\delta\mathbf{u}^i/\langle|\delta\boldsymbol{u}^i|\rangle$, so that $\langle|\delta\varphi^i|\rangle=1$. The correlation function was defined as: $C(r)=\langle\delta\varphi^i\cdot\delta\varphi^j\,\delta(r-D^{i,j})\rangle/\langle\delta(r-D^{i,j})\rangle$, where $D^{i,j}$ is the distance between birds i and j, and the symbol · denotes an inner product. Since $C(r)$ decreases linearly to zero with increasing r and becomes negative for even larger r (Fig. 4b), we can define the correlation length r_0 as $C(r=r_0)=0$[23].

Self-propelled particle model. To test whether the observed trends in our empirical data (Fig. 4c) applied to general biological systems containing pair-bonded individuals and unpaired embedded within groups, we modified the simple flocking model developed by Vicsek *et al*. (1995)[3]. In this model, N self-propelled particles move at the same speed $|\boldsymbol{u}_0|$ and align their directions of motion to the average velocity of the neighbours within a *metric* perception range, with some noise added. The noise was a random number chosen with a uniform probability from the interval $[-\tau/2, \tau/2]$. We modified the Vicsek model by using a *topological* interaction, where each particle interacted with a fixed number of neighbours instead of all neighbours within a certain *metric* distance. To account for the effect of social relationships, we let same particles interact with 3 neighbours and others interact with 7 neighbours. We also added a repulsion zone[54] (with radius r_0) for every particle to prevent particles from forming locally dense clusters. We ran the simulation on a two-dimensional square box of length S with periodic boundary conditions and with a time step Δt. Particle density was defined as $\rho=N/S^2$. The parameters were chosen as: $|\boldsymbol{u_0}|=1$ m/s, $\tau=0.3$, $r_0=0.2/\rho^{0.5}$, $\Delta t=0.1$ s, $\rho=2$ m^{-2} and $S=25$ m. The noise level was selected to produce group polarizations similar to those observed in the experiment. We initialized the simulations by setting all the particles to be moving in the same direction. After more than 100 time steps, the simulation was stable with particles moving in a new common direction except for tiny fluctuations between individuals (Supplementary Fig. 12a-c). For each P_{paired}, we selected 100 time frames between steps 1,000 and 10,000 at an interval of $100\Delta t$, and repeated this procedure 6 times to obtained a total of 600 frames. To avoid contamination from the periodic boundary conditions, we only used particles near the centre of the simulation domain (with diameter of $2S/3$) to calculate correlation length. Sample correlation functions for different levels of P_{paired} are shown in Supplementary Fig. 12d.

Ethics statement. To ensure that birds were not disturbed, a researcher controlled the laptop and function generator from within a hide, and could not be seen by birds flying overhead. All field protocols were approved by the Biosciences Ethics Panel of the University of Exeter (ref 2017/2080) and adhered to the Association for the Study of Animal Behaviour Guidelines for the Treatment of Animals in Behavioural Research and Teaching.

Data availability. Supplementary Figures 1 to 12 and Supplementary Tables 1 to 3 are available in the Supplementary Information. Raw images captured by one of the four cameras and the reconstructed birds'

3D movement trajectories are provided in Supplementary Videos 1 to 6. Plain text files, each including bird ID number, position, time, velocity, acceleration, and wingbeat frequency at every time step are provided in Supplementary Data 1 to 7. A plain text file that includes mean wingbeat frequency, flight speed, and local density (approximated by the number of neighbours within a distance of 5 m from the focal bird) for paired and unpaired birds in six flocks as well as for birds flying alone are provided in Supplementary Data 8. All data required to produce results in this study are included in Supplementary Data 1 to 8. Supplementary Data and Supplementary Videos are available at https://figshare.com/s/c55eb82bab800571d25d.

Reference

1. Biro, D., Sasaki, T. & Portugal, S. J. Bringing a Time–Depth Perspective to Collective Animal Behaviour. *Trends Ecol. Evol.* **31,** 550–562 (2016).
2. Sumpter, D. J. T. The principles of collective animal behaviour. *Philos. Trans. R. Soc. B Biol. Sci.* **361,** 5–22 (2006).
3. Vicsek, T., Czirók, A., Ben-Jacob, E., Cohen, I. & Shochet, O. Novel Type of Phase Transition in a System of Self-Driven Particles. *Phys. Rev. Lett.* **75,** 1226–1229 (1995).
4. Vicsek, T. & Zafeiris, A. Collective motion. *Phys. Rep.* **517,** 71–140 (2012).
5. Croft, D., James, R. & Krause, J. *Exploring Animal Social Networks*. (Princeton University Press, 2008).
6. del Mar Delgado, M. *et al.* The importance of individual variation in the dynamics of animal collective movements. *Philos. Trans. R. Soc. B Biol. Sci.* **373,** 20170008 (2018).
7. King, A. J., Fehlmann, G., Biro, D., Ward, A. J. & Fürtbauer, I. Re-wilding Collective Behaviour: An Ecological Perspective. *Trends Ecol. Evol.* **33,** 347–357 (2018).
8. Farine, D. R., Strandburg-Peshkin, A., Couzin, I. D., Berger-Wolf, T. Y. & Crofoot, M. C. Individual variation in local interaction rules can explain emergent patterns of spatial organization in wild baboons. *Proc. R. Soc. B Biol. Sci.* **284,** 20162243 (2017).
9. Bode, N. W. F., Wood, A. J. & Franks, D. W. Social networks and models for collective motion in animals. *Behav. Ecol. Sociobiol.* **65,** 117–130 (2011).

10. Krause, J., James, R., Franks, D. & Croft, D. *Animal Social Networks*. (Oxford University Press, 2015).

11. Jolles, J. W., King, A. J., Manica, A. & Thornton, A. Heterogeneous structure in mixed-species corvid flocks in flight. *Anim. Behav.* **85,** 743–750 (2013).

12. King, A. J., Sueur, C., Huchard, E. & Cowlishaw, G. A rule-of-thumb based on social affiliation explains collective movements in desert baboons. *Anim. Behav.* **82,** 1337–1345 (2011).

13. Moussaïd, M., Perozo, N., Garnier, S., Helbing, D. & Theraulaz, G. The walking behaviour of pedestrian social groups and its impact on crowd dynamics. *PLoS One* **5,** 1–7 (2010).

14. Hemelrijk, C. K. & Kunz, H. Density distribution and size sorting in fish schools: an individual-based model. *Behav. Ecol.* **16,** 178–187 (2005).

15. Sueur, C., Petit, O. & Deneubourg, J. L. Short-term group fission processes in macaques: a social networking approach. *J. Exp. Biol.* **213,** 1338–1346 (2010).

16. Bode, N. W. F., Wood, A. J. & Franks, D. W. The impact of social networks on animal collective motion. *Anim. Behav.* **82,** 29–38 (2011).

17. Miguel, M. C., Parley, J. T. & Pastor-Satorras, R. Effects of Heterogeneous Social Interactions on Flocking Dynamics. *Phys. Rev. Lett.* **120,** 068303 (2018).

18. Farine, D. R. *et al.* Both nearest neighbours and long-term affiliates predict individual locations during collective movement in wild baboons. *Sci. Rep.* **6,** 1–10 (2016).

19. Black, J. *Partnerships in Birds: the Study of Monogamy*. (Oxford University Press, 1996).

20. Hemelrijk, C. K. & Hildenbrandt, H. Scale-Free Correlations, Influential Neighbours and Speed Control in Flocks of Birds. *J. Stat. Phys.* **158,** 563–578 (2014).

21. Hemelrijk, C. K. & Hildenbrandt, H. Some Causes of the Variable Shape of Flocks of Birds. *PLoS One* **6,** e22479 (2011).

22. Ballerini, M. *et al.* Interaction ruling animal collective behavior depends on topological rather than metric distance: Evidence from a field study. *Proc. Natl. Acad. Sci.* **105,** 1232–1237 (2008).

23. Cavagna, A. *et al.* Scale-free correlations in starling flocks. *Proc. Natl. Acad. Sci.* **107,** 11865–11870 (2010).

24. Emery, N. J., Seed, A. M., Von Bayern, A. M. P. & Clayton, N. S. Cognitive adaptations of social bonding in birds. *Philos. Trans. R. Soc. B Biol. Sci.* **362,** 489–505 (2007).

25. Kubitza, R. J., Bugnyar, T. & Schwab, C. Pair bond characteristics and maintenance in free-flying jackdaws

Corvus monedula: Effects of social context and season. *J. Avian Biol.* **46,** 206–215 (2015).

26. Röell, A. Social behaviour of the jackdaw, Corvus monedula , in relation to its niche. *Behaviour* **64,** 1–124 (1978).

27. Valletta, J. J., Torney, C., Kings, M., Thornton, A. & Madden, J. Applications of machine learning in animal behaviour studies. *Anim. Behav.* **124,** 203–220 (2017).

28. Kings, M. Foraging tactics and social networks in wild jackdaws. *Ph.D. thesis* (University of Exeter, 2018).

29. Ling, H. *et al.* Simultaneous measurements of three-dimensional trajectories and wingbeat frequencies of birds in the field. *J. R. Soc. Interface* **15,** 20180653 (2018).

30. Katz, Y., Tunstrom, K., Ioannou, C. C., Huepe, C. & Couzin, I. D. Inferring the structure and dynamics of interactions in schooling fish. *Proc. Natl. Acad. Sci.* **108,** 18720–18725 (2011).

31. Usherwood, J. R., Stavrou, M., Lowe, J. C., Roskilly, K. & Wilson, A. M. Flying in a flock comes at a cost in pigeons. *Nature* **474,** 494–497 (2011).

32. Tobalske, B. W., Hedrick, T. L., Dial, K. P. & Biewener, A. A. Comparative power curves in bird flight. *Nature* **421,** 363–366 (2003).

33. Chen, X., Dong, X., Be'Er, A., Swinney, H. L. & Zhang, H. P. Scale-invariant correlations in dynamic bacterial clusters. *Phys. Rev. Lett.* **108,** 148101 (2012).

34. Cavagna, A., Giardina, I. & Grigera, T. S. The physics of flocking: Correlation as a compass from experiments to theory. *Phys. Rep.* **728,** 1–62 (2018).

35. Couzin, I. D., Krause, J., Franks, N. R. & Levin, S. A. Effective leadership and decision-making in animal groups on the move. *Nature* **433,** 513–516 (2005).

36. Woods, R. D., Kings, M., McIvor, G. E. & Thornton, A. Caller characteristics influence recruitment to collective anti-predator events in jackdaws. *Sci. Rep.* **8,** 1–8 (2018).

37. Kondo, N., Izawa, E.-I. & Watanabe, S. Crows cross-modally recognize group members but not non-group members. *Proc. R. Soc. B Biol. Sci.* **279,** 1937–1942 (2012).

38. Henderson, I. G., Hart, P. J. B. & Burke, T. Strict Monogamy in a semi-colonial Passerine: the jackdaw Corvus monedula. *J. Avian Biol.* **31,** 177–182 (2000).

39. Henderson, I. G. & Hart, P. J. B. Provisioning, parental investment and reproductive success in Jackdaws Corvus monedula. *Ornis Scand.* **24,** 142–148 (1993).

40. Coombs, C. J. F. Rookeries and roosts of the rook and jackdaw in south-west cornwall. *Bird Study* **8,** 55–70 (1961).

41. Zandberg, L., Jolles, J. W., Boogert, N. J. & Thornton, A. Jackdaw nestlings can discriminate between conspecific calls but do not beg specifically to their parents. *Behav. Ecol.* **25,** 565–573 (2014).

42. Aubin, T. & Jouventin, P. Cocktail party effect in king penguin colonies. *Proc. R. Soc. B* **265,** 1665–1673 (1998).

43. Kondo, N., Izawa, E.-I. & Watanabe, S. Crows cross-modally recognize group members but not non-group members. *Proc. R. Soc. B* (2012). doi:10.1098/rspb.2011.2419

44. Hartley, R. & Zisserman, A. *Multiple view geometry in computer vision*. *Cambridge University Press* (2004). doi:10.1007/s13398-014-0173-7.2

45. Theriault, D. H. *et al.* A protocol and calibration method for accurate multi-camera field videography. *J. Exp. Biol.* **217,** 1843–1848 (2014).

46. Furukawa, Y. & Ponce, J. Accurate camera calibration from multi-view stereo and bundle adjustment. *Int. J. Comput. Vis.* **84,** 257–268 (2009).

47. Ouellette, N. T., Xu, H. & Bodenschatz, E. A quantitative study of three-dimensional Lagrangian particle tracking algorithms. *Exp. Fluids* **40,** 301–313 (2006).

48. Ouellette, N. T., Xu, H., Bourgoin, M. & Bodenschatz, E. An experimental study of turbulent relative dispersion models. *New J. Phys.* **8,** (2006).

49. Kelley, D. H. & Ouellette, N. T. Emergent dynamics of laboratory insect swarms. *Sci. Rep.* **3,** 1073 (2013).

50. Mordant, N., Crawford, A. M. & Bodenschatz, E. Experimental Lagrangian acceleration probability density function measurement. *Phys. D Nonlinear Phenom.* **193,** 245–251 (2004).

51. Puckett, J. G., Ni, R. & Ouellette, N. T. Time-Frequency Analysis Reveals Pairwise Interactions in Insect Swarms. *Phys. Rev. Lett.* **114,** 258103 (2015).

52. Cavagna, A., Queiros, S. M. D., Giardina, I., Stefanini, F. & Viale, M. Diffusion of individual birds in starling flocks. *Proc. R. Soc. B Biol. Sci.* **280,** 20122484 (2013).

53. Attanasi, A. *et al.* Collective Behaviour without Collective Order in Wild Swarms of Midges. *PLoS Comput. Biol.* **10,** e1003697 (2014).

54. Couzin, I. D., Krause, J., James, R., Ruxton, G. D. & Franks, N. R. Collective Memory and Spatial Sorting

in Animal Groups. *J. Theor. Biol.* **218,** 1–11 (2002).

Acknowledgements

This work was supported by a Human Frontier Science Program grant to AT, NTO and RTV, Award Number RG0049/2017. We are grateful to Paul Dunstan, Richard Stone, and the Gluyas family for permission to work on their land, and to Victoria Lee, Beki Hooper, Amy Hall, Paige Petts, Christoph Peterson, and Joe Westley for their assistance in the field.

Authors' contributions

H.L., N.T.O, A.T. and R.T.V. conceived the ideas; H.L. and N.T.O. designed the methodology; G.M. and A.T. collected the data; H.L., K.V. and N.T.O analysed the data; G.M., H.L. and A.T. performed statistical analysis; and All led the writing of the manuscript. All authors contributed critically to the drafts and gave final approval for publication.

Competing interests

We declare we have no competing interests.

Additional information

Supplementary information is available for this paper at http://doi.org/#

Reprints and permissions information is available at http://www.nature.com/ reprints.

Correspondence and requests for materials should be addressed to N.T.O and A.T.